NURETH14-337

Hydraulic Benchmark Data for PWR Mixing Vane Grid

M. E. Conner¹, Elvis E. Dominguez-Ontiveros², Yassin A. Hassan²

¹Westinghouse Electric Company LLC, Columbia, SC, USA

²Nuclear Engineering Department, Texas A&M University, College Station, TX

<u>connerme@westinghouse.com</u>

Abstract

The purpose of the present study is to present new hydraulic benchmark data obtained for PWR rod bundles for the purpose of benchmarking Computational Fluid Dynamics (CFD) models of the rod bundle. The flow field in a PWR fuel assembly downstream of structural grids which have mixing vane grids attached is very complex due to the geometry of the subchannel and the high axial component of the velocity field relative to the secondary flows which are used to enhance the heat transfer performance of the rod bundle. Westinghouse has a CFD methodology to model PWR rod bundles that was developed with prior benchmark test data. As improvements in testing techniques have become available, further PWR rod bundle testing is being performed to obtain advanced data which has high spatial and temporal resolution. This paper presents the advanced testing and benchmark data that has been obtained by Westinghouse through collaboration with Texas A&M University.

Introduction

As the demand on PWR fuel has increased since the mid 1990's due to longer cycles and power uprates, the thermal conditions during normal operation have become more limiting. Unexpected crud deposition due to local subcooled boiling has led to axial power shifts and localized corrosion. These problems have resulted in mitigation steps being taken at the PWR plants which reduce the efficiency of the fuel. If local conditions in the PWR core could be better predicted, these problems can be avoided.

Advancements in analytical methods have occurred since the late 1990's to improve the prediction of the local thermal-hydraulic conditions. One method utilized in PWR fuel is the use of Computational Fluid Dynamics (CFD) to predict flow and temperature in the flow downstream of grids with mixing vanes. Benchmarking of the CFD models has been performed with the available data to provide a reasonable prediction. As advancements in both computational speed and data acquisition methods have improved dramatically over recent years, there is opportunity to further improve the CFD model methodology and provide closer predictions to PWR conditions.

This paper discusses the advanced hydraulic data obtained on Westinghouse PWR mixing vane grids at Texas A&M University. The test bundle, test loop, and data acquisition will be discussed in the paper. The data acquisition of interest is from an advanced Particle Image Velocimetry (PIV) technique which can get high spatial and temporal resolution of the velocity vectors. The quality of the data represents a step-change improvement from the prior data used to benchmark the CFD methodology. Details of this data will be presented in the paper.

1. Background

Since the mid 1990's, Westinghouse has been developing and improving a CFD modeling methodology for PWR rod bundles. A summary of this prior benchmark data is provided here.

PWR fuel assemblies are vertical rod bundles which have flow moving from the bottom of the fuel to the top. The rod bundles have structural grids, spaced at specific axial distances, that support the long, vertical fuel rods and maintain the appropriate fuel rod pitch. Mixing vanes are swirl generators that are placed on the top (downstream) edge of the structural grids to improve the critical heat flux (CHF) performance of the fuel assembly. These mixing vanes also improve the heat transfer in the rod bundle during normal PWR operation. Figure 1 shows some PWR fuel assemblies, a structural grid, and a sub-model of a structural grid which has mixing vanes.

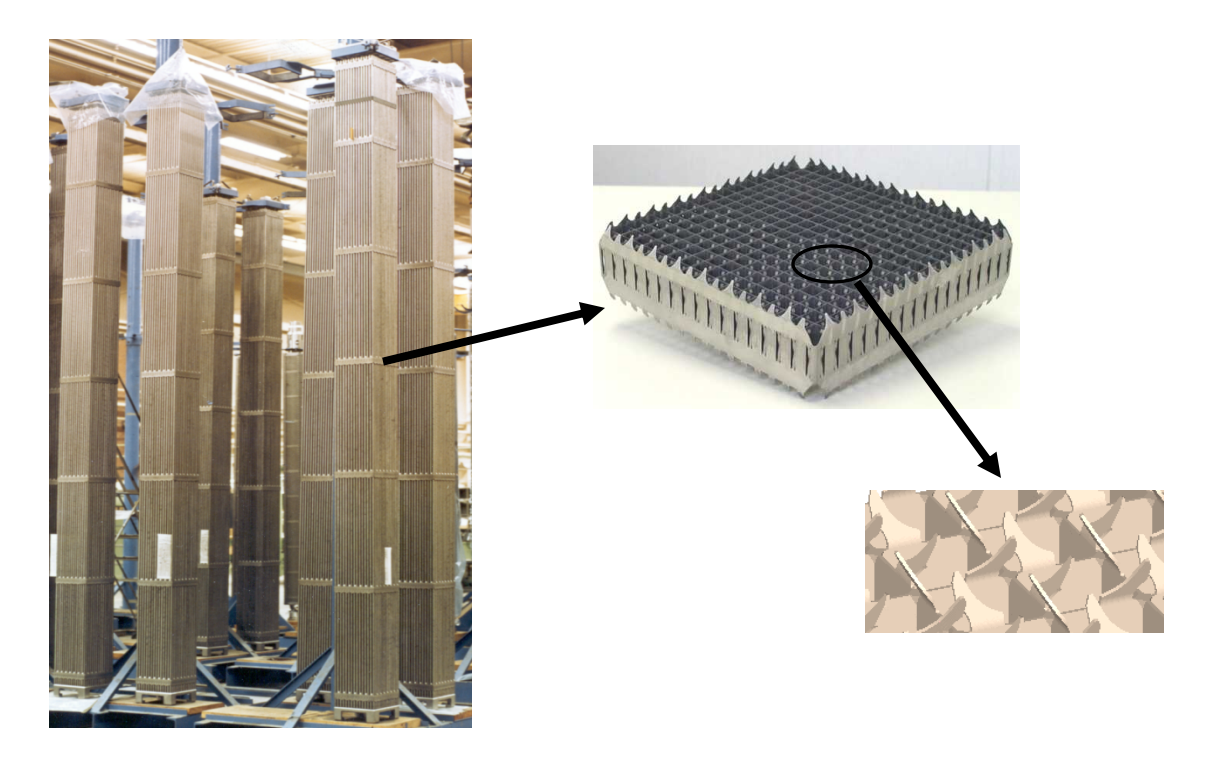


Figure 1: PWR Rod Bundle / Structural Grid / Mixing Vanes

The mixing vanes provide secondary flow structures (swirl, crossflow) that increase the mixing and turbulence in the rod bundle. This turbulence/mixing/swirl is very strong just downstream of the mixing vanes, and it decays as the flow travels downstream of the mixing vanes. Predicting this lateral flow field downstream of the grid with CFD is very challenging and requires good data for benchmarking.

1.1 Prior Benchmark Data

Westinghouse had a long time collaboration with Clemson University on rod bundle hydraulic and heat transfer testing. The purpose of this collaboration was to study the effect of mixing vanes on the flow and heat transfer in PWR rod bundles. The data collected during that collaboration was used to benchmark a CFD modeling methodology for PWR rod bundles.

Particle Image Velocimetry (PIV) was use to study the lateral velocity vectors downstream of the the grids with mixing vanes [1] [2]. Figure 2 provides an example of the PIV data obtained from this testing.

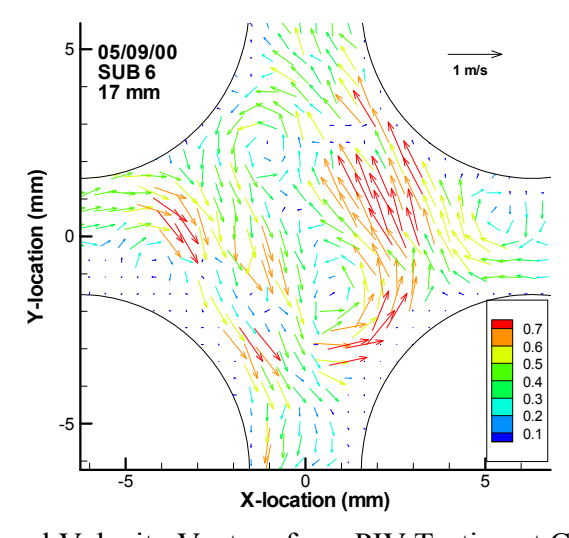


Figure 2: Lateral Velocity Vectors from PIV Testing at Clemson University

Heat transfer testing was also part of the prior benchmark testing. The heat transfer testing included local average heat transfer measurements [3], local azimuthal heat transfer measurements [4], and heat transfer measurements using fully heated rods [5].

A multi-year project was completed which developed and benchmarked a CFD modeling methodology for PWR rod bundles using all of the available data. The methodology has been discussed at prior technical meetings [6].

1.2 Westinghouse / Texas A&M Collaboration

Currently, Westinghouse and Texas A&M are collaborating on PWR hydraulic testing. One driver for getting new hydraulic benchmark data for PWR rod bundles is the large improvements in PIV testing techniques which allow for high spatial and temporal resolution. The main improvement has been in the high-speed cameras, which had rapid improvements in the early 2000s. These cameras can now record 7,500 to 30,000 frames per second (fps) with high-temporal and high-spatial resolutions [7].

Initial test results from PIV testing at Texas A&M were presented last fall at the CFD4NRS-3 workshop [8]. Building upon the work reported in that paper, an improved test facility has been prepared at Texas A&M for this PWR rod bundle testing. Initial results from this new test facility are reported in the current paper.

2. Test Facility

As noted in Section 1.2 above, an improved test facility at Texas A&M has been built. The test facility offers improvements over the prior test facility which will allow for higher Reynolds Number testing, as well as allowing optical access for lateral plane PIV data acquisition. Additionally, a new flow housing was built for this test facility which removes the bypass region which was present in the prior flow housing [8].

2.1 Test Loop

The test loop is a basic hydraulic test loop with a tank, pump, flow meter, and test section. The test loop has been design so that the test section is vertical, with flow moving from bottom to top, consistent with actual fuel bundles. The pump and loop have been sized to allow for higher Reynolds Number testing than the prior facility [8]. This will allow data acquisition to take place at a Reynolds Number (Re = 28,000) consistent with prior hydraulic testing [1] [2]. Note that the test loop can achieve much higher Reynolds Numbers.

An independent check of the flow meter reading has been performed by taking axial PIV data (see Section 2.4) in the flow housing with no rods installed. This check confirmed that the flow meter and PIV are provided consistent flow measurements.

2.2 Test Bundle

The test bundle is a 5×5 rod bundle which is representative of a 17×17 fuel assembly design. The rod bundle pitch (12.6 mm), rod diameter (9.5 mm), and grid features (rod support features, mixing vane) are identical to a 17×17 fuel assembly. The only reduction in scale is in the overall array size versus a 17×17 array. There are 25 rods in the test bundle, with no thimble tube (i.e., larger diameter structural support tube) locations in the 5x5 rod bundle.

The test bundle consists of multiple grids, spaced on a typical axial grid spacing of 510 mm. The grids have mixing vanes on them. Figure 3 provides a 3-D view of the test grids. There are locations in the test bundle, away from measurement regions, where non-vaned support grids are used.

The test rods used in the test bundle were fabricated using a fluorinated ethylene-propylene (FEP) plastic with dimensions of 9.5 OD x 9 ID x 1270 mm long with a +-0.0762 mm tolerance in all dimensions. This tube material was chosen to match the refractive index of water.

Therefore, these tubes are optically transparent when immersed in water during testing. For reinforcement away from the measurement region, thick tubes of a different plastic were inserted from the top and bottom inside the FEP tubes to maintain rod rigidity during testing. This ensures that the rods are maintaining the appropriate rod pitch in the ungridded regions and are not vibrating under flow conditions.

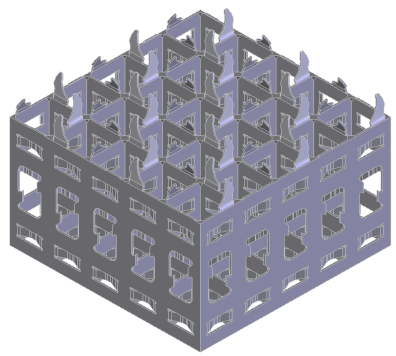


Figure 3: 5x5 Test Grid with Mixing Vanes

2.3 Flow Housing

A new flow housing was built for this test facility. The housing is a square, with a small gap between the grids and the housing inner walls. The walls are made out of transparent acrylic to allow for optical transparency for the laser and the camera. Pressure taps are located on the housing walls so that pressure drop over different regions of the test bundle can be acquired.

The flow entering into the bottom of the housing has been conditioned so that it is essentially pure vertical flow. This is accomplished by the design of the loop below the housing. The vertical flow from the pump is directed into a plenum region where the flow maintains its axial direction. The plenum region reduces in cross-section area as the flow travels toward the housing. The flow travels through a flow straightener and eventually into the bottom of the flow housing.

2.4 Data Acquisition

Data acquisition includes pressure drop measurements and velocity vector measurements.

2.4.1 Velocity Vector Measurements

The primary measurements are the velocity vectors. These measurements are made using an advanced Particle Image Velocimetry (PIV) technique which can get high spatial and temporal resolution of the velocity vectors. The technique used is two-dimensional Time Resolved Particle Image Velocimetry (TR-PIV). This technique is discussed in detail in Reference [8].

PIV data is taken in two configurations. The first configuration is with the laser setup for axial planes in the rod bundle. The configuration is similar to the data acquisition in the prior test facility [8]. The second configuration is with the laser setup for lateral planes in the rod bundle.

The PIV data can be used in various ways. The images can be used for flow visualization (i.e., without data reduction). After data reduction, average or instantaneous flow fields can be looked at for comparison with CFD results.

A schematic showing the data acquisition setup is provided in Figure 4. Also included in this figure is a picture of the flow housing.

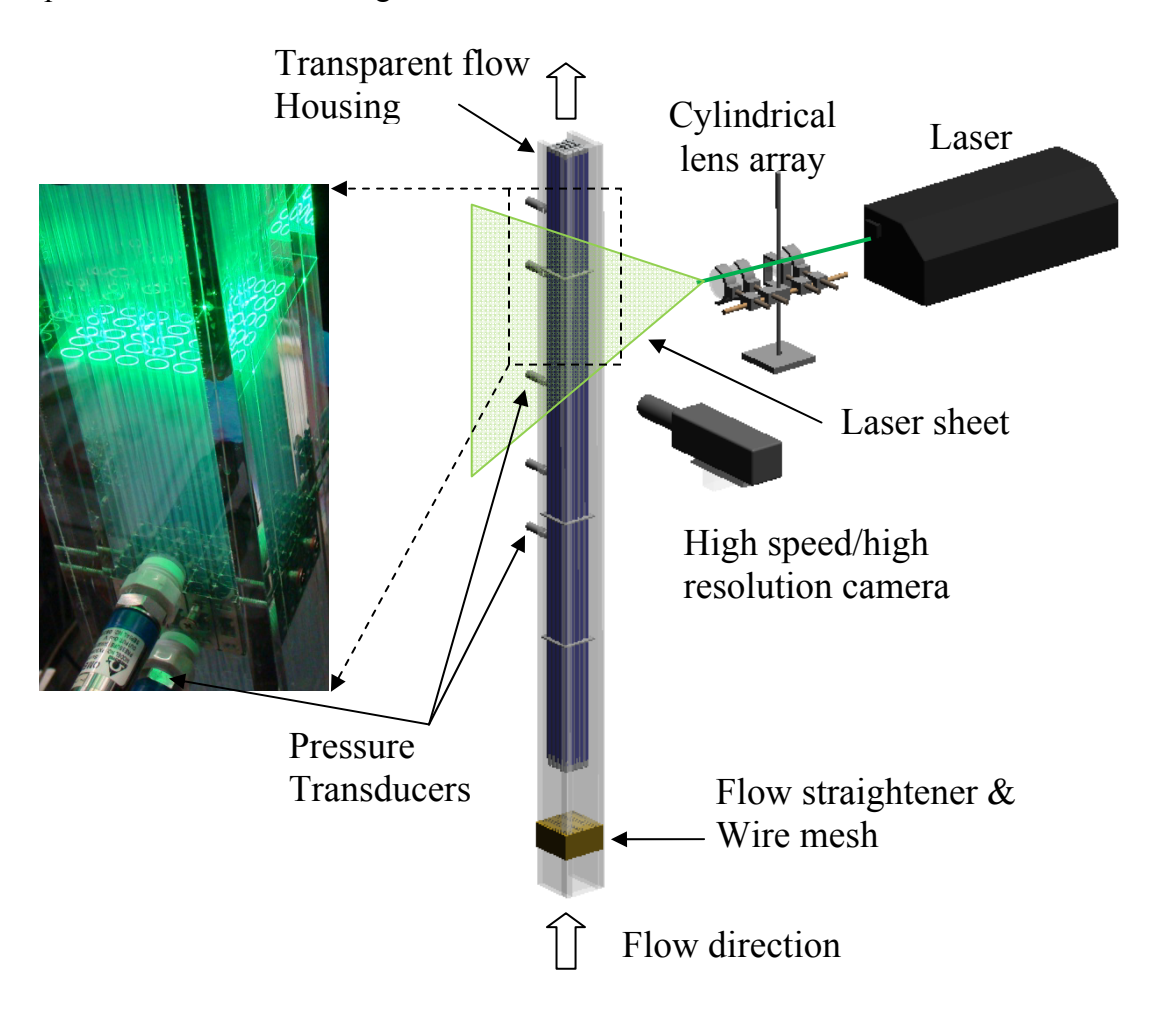


Figure 4: Schematic of Data Acquisition

3. Results

The data acquired from this testing include pressure drop measurements and velocity vector measurements. The pressure drop data from this testing is consistent with pressure drop measured in other test facilities. The focus of the results presentation will be on the measurement velocity vectors using the TR-PIV technique.

The measurements for axial and lateral velocity at the investigated region were performed at several planes using a multi-scale approach. This approach consisted of performing

measurements on various viewing areas of the test section. The scales were selected based on the physical constrictions and the desired resolution of the velocity fields.

3.1 Axial Velocity Results

3.1.1 Full Field Velocity Results

In this section, the focus is on two adjacent planes located in the vicinity of the rod bundle middle plane. The location of the physical center of the bundle lies in a line that crosses the diameter of the central rods. The measurements were performed at the plane formed by the bundle center and an adjacent plane. Figure 5 shows a photographic image of the test section viewing area. The dimensions of the viewing area are 67 mm in length along the X-axis direction and 51 mm height along the axial flow direction (Y-axis). At the bottom of Figure 5, the mixing vanes of the grid can be seen. The physical locations of the plastic cylinders representing the fuel rods are shown with a dotted line for better appreciation. Since the plastic rods match the refractive index of the water used as working fluid, the rods "disappear" in the test section. The position of the plane of view is shown on the right top corner which is located at the physical center of the rod for this particular case (Plane 6).

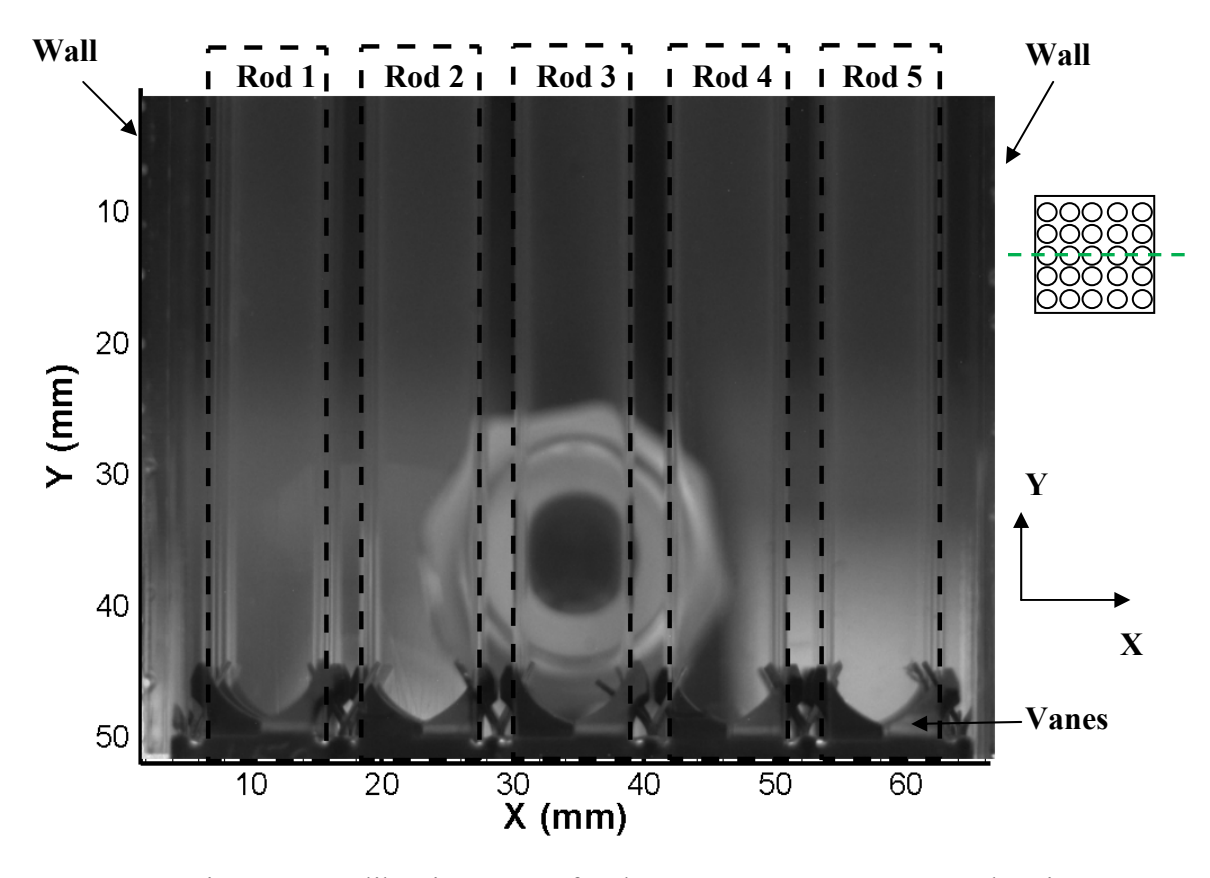


Figure 5: Calibration Image for the PIV Measurement Area Showing the Location of Rods and Mixing Vanes.

Figure 6 shows the average velocity vector field obtained under a Re number condition of 28,000 for Plane 7. The position of Plane 7 is shown on the right top corner of Figure 6; Plane 7 represents a plane through the rod gaps, and it is parallel to Plane 6. The color of each vector represents the axial component of the measured velocity at each location inside the measurement area. The effect of the mixing vane is observed by a deflection in the flow creating a swirl that evolves in the axial direction. The major flow direction is indicated with white color arrows.

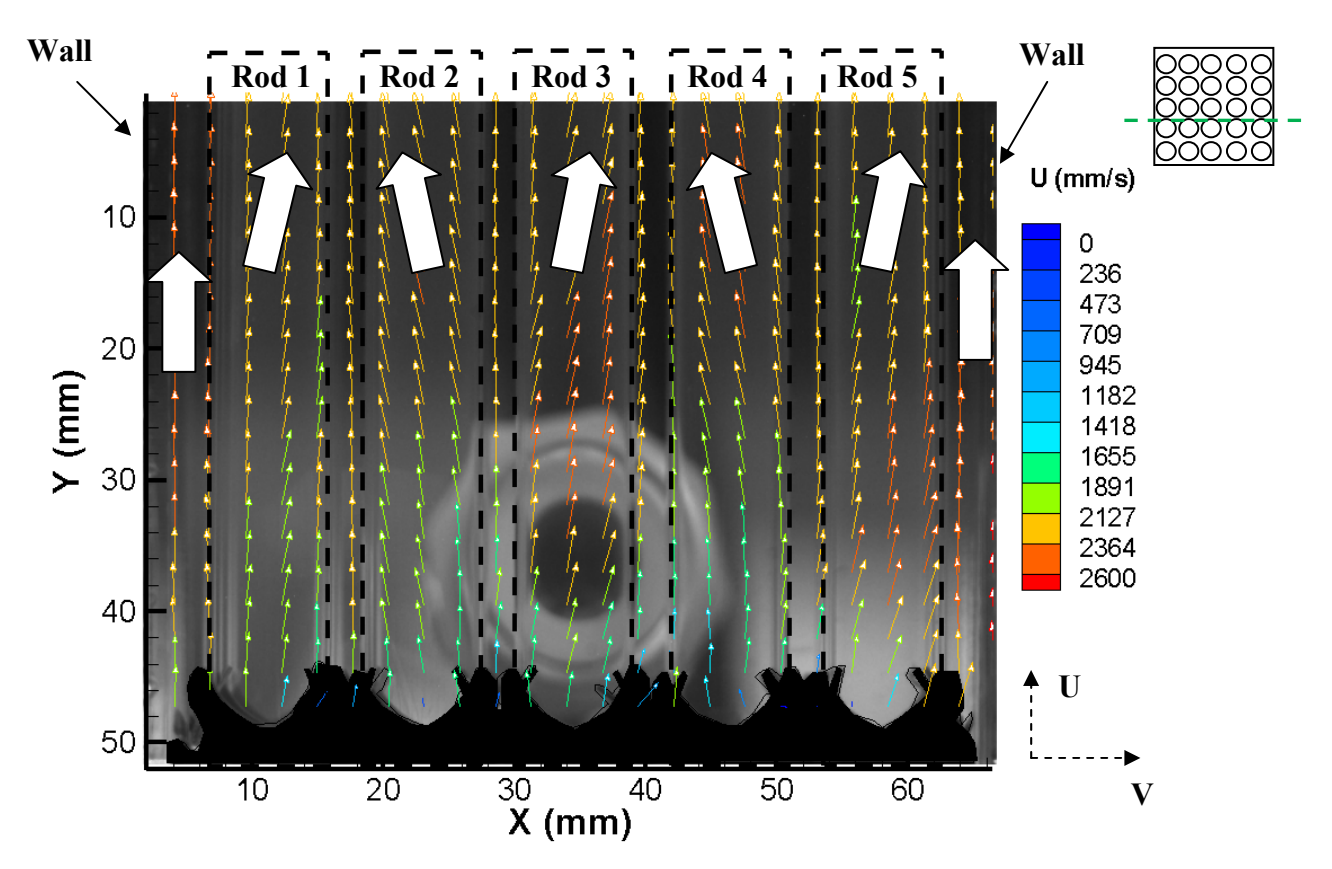


Figure 6: Averaged Velocity Vector Field, Re=28,000 at Plane 7

The velocity magnitude of each component of the velocity vector is represented in a contour plot for measured positions upstream and downstream the grid in the figures below. Figure 7 shows the axial velocity component in Plane 7. It should be appreciated that the swirling flow created by the vanes have three-dimensional structures. Therefore, flow reductions in one part of the flow field are accompanied by flow increases elsewhere in the flow field (perhaps on a different plane) to ensure mass conservation. Therefore, the unexpected axial velocity plot in Figure 7 (velocity decrease just downstream of the grid) means that there is a velocity increase downstream of grid in other planes that are not measured or shown in this paper.

The axial flow velocity on Plane 7 is considerably modified downstream the grid showing a zone of velocity reduction nearby the mixing vanes with zones of higher velocity gradient at the bundle central sub-channels. A zone of important axial velocity reduction is highlighted using a red dotted oval. This zone shows a reduction of the axial velocity of about 20% with

respect to the axial velocity upstream the grid. The velocity gradient is well delineated starting at a low velocity (blue contour colour) nearby the vanes and increasing along the axial distance from the grid. The contour plot shows that the highest axial velocity gradient area is restricted to a distance in the axial direction of 30 mm from the base of the grid. The current measurements were performed using a 2-D PIV system, therefore only two components of the velocity vector can be measured at the time. However, the lateral component of the velocity vector shown in Figure 8 clearly shows an increase in the lateral velocity component downstream the grid.

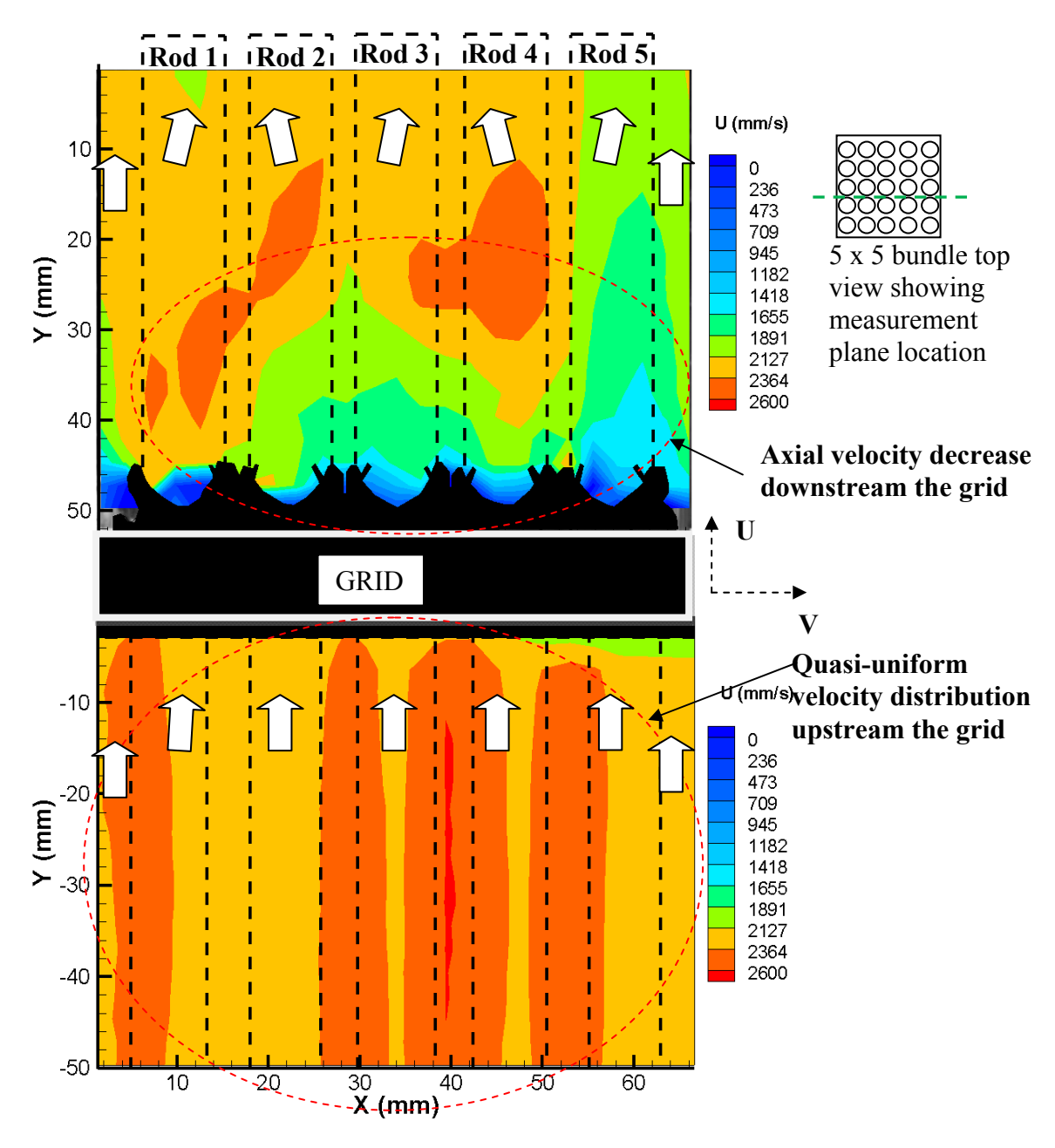


Figure 7: Axial Velocity Evolutions Upstream and Downstream the Grid (Re=28,000, Plane 7)

The increase in the lateral velocity shown in Figure 8 denoted by the contour plot is driven by the vane orientation. The flow is deflected following the vane orientation causing the lateral velocity increase. The maximum magnitude of the increase is about 20% of the axial component. The white arrows in the figure denote the main flow direction. Since the flow is diverted by the vanes from a straight vertical path, a cross flow is induced in the bundle.

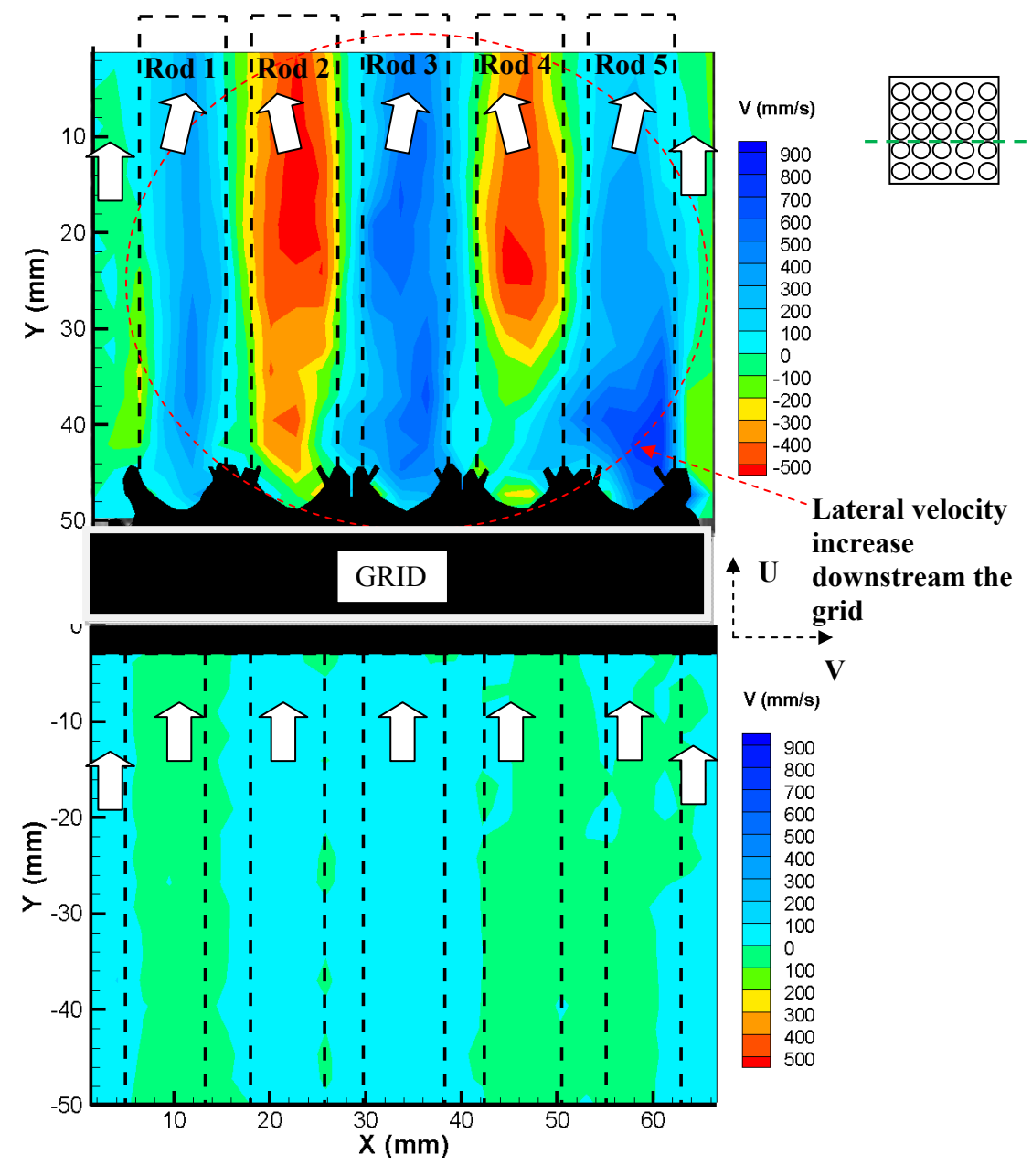


Figure 8: Lateral Velocity Evolution Upstream and Downstream the Grid (Re=28,000, Plane 7)

This cross flow is induced by the vanes' orientation and the geometry surrounding the grid. Figure 9 shows the evolution of the axial velocity for the central plane of the bundle. The

velocity fields in the two axial planes of interest (Plane 6 and Plane 7) can be compared. The axial velocity in Figure 9 follows a similar trend of the one showed in Figure 7. The axial velocity in the region close to the grid decreases.

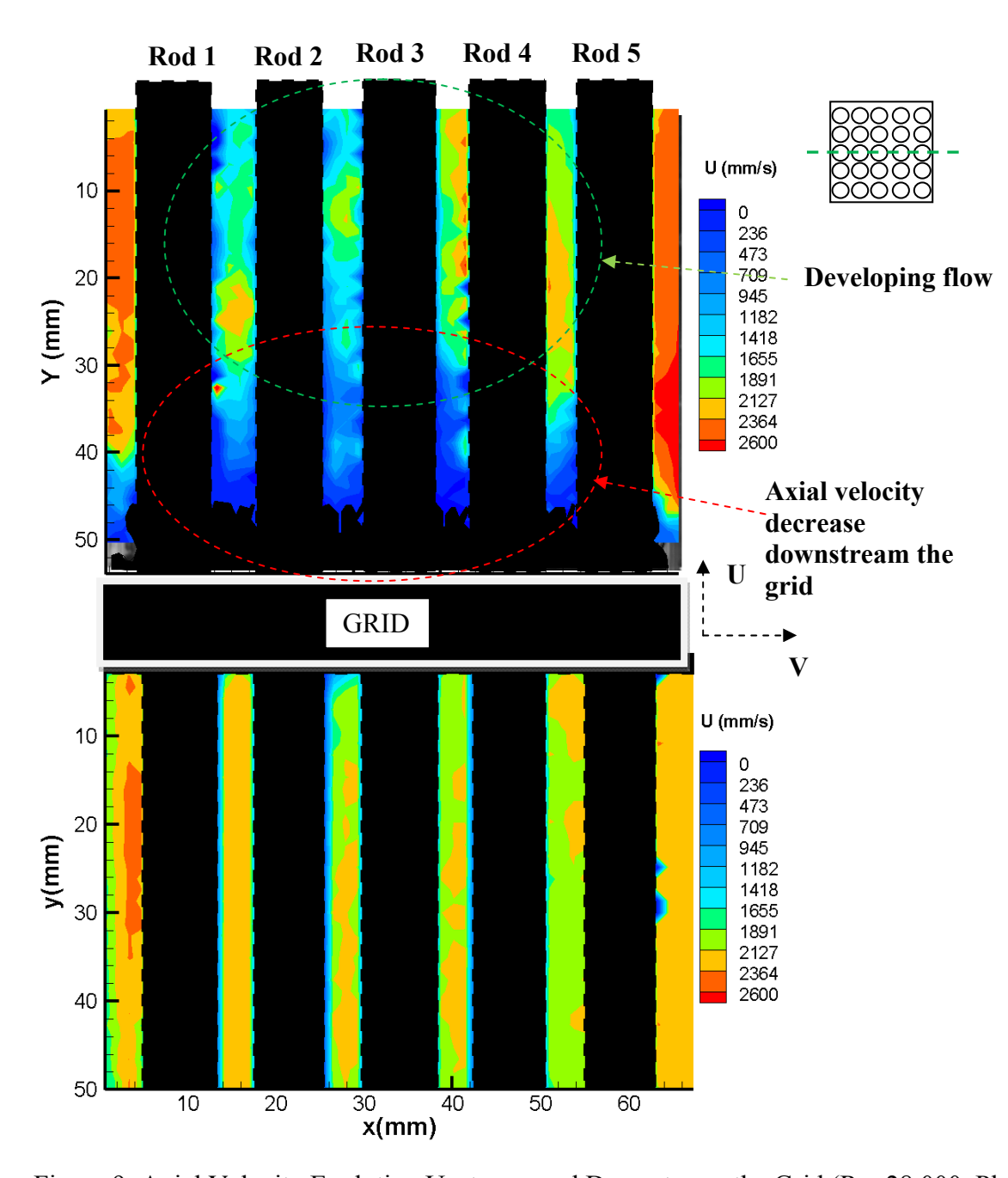


Figure 9: Axial Velocity Evolution Upstream and Downstream the Grid (Re=28,000, Plane 6)

The flow in Figure 9 shows a more uniform axial velocity distribution for a distance of 30 mm in the axial direction from the base of the grid denoted by the red dotted oval when compared to the same region in Figure 7. However, the flow develops slowly after this region showing a

steeper velocity gradient for the regions inside the green dotted oval in Figure 9. The flow downstream the grid in Figure 9 show zones of low and high velocity in a short spatial area.

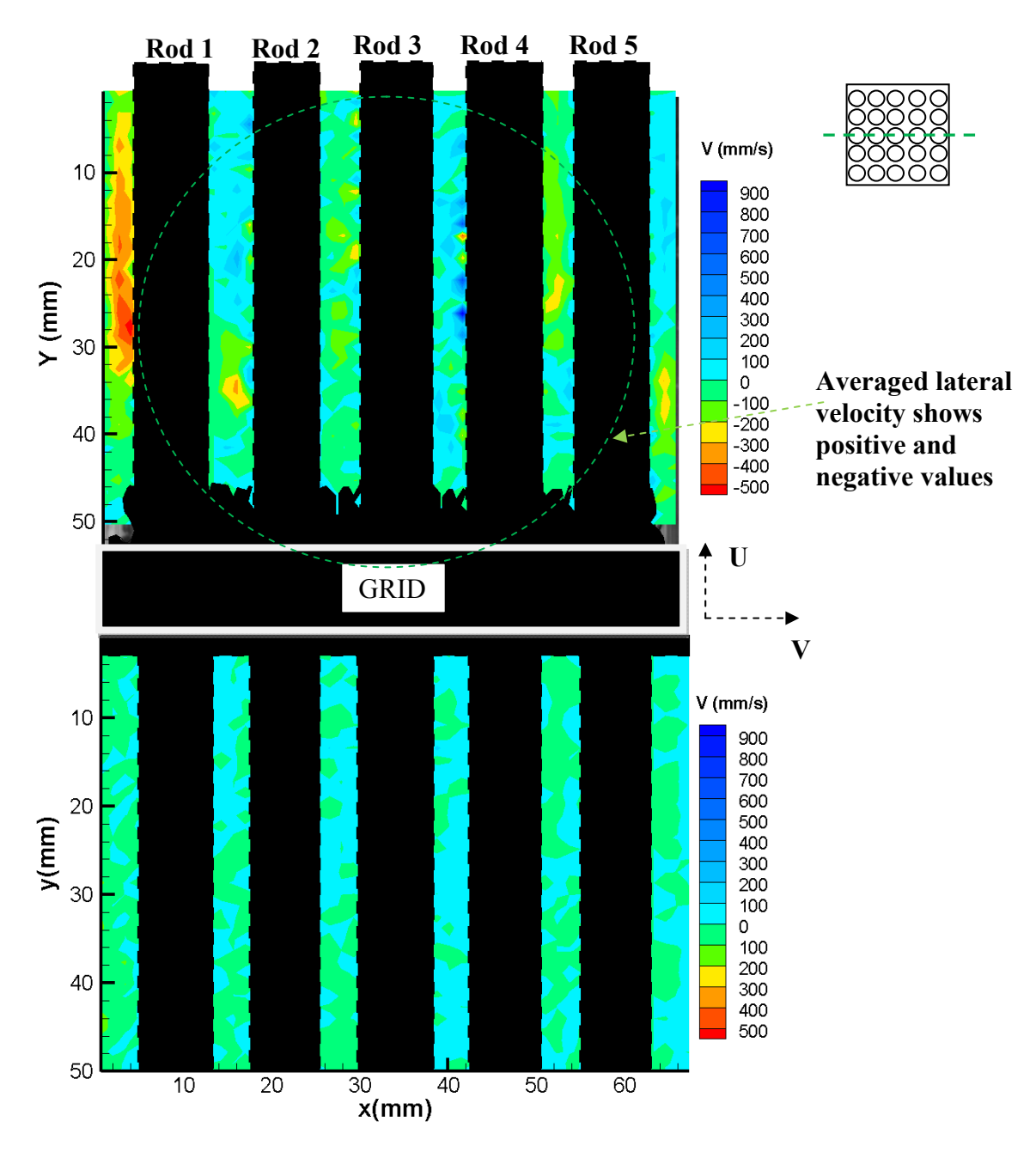


Figure 10: Lateral Velocity Evolutions Upstream and Downstream the Grid (Re=28,000, Plane 6)

Observation of the behaviour of the lateral component in Plane 6 shows a switch between positive and negative values of the lateral velocity along the axial direction denoted by areas of blue contour colour alternating with areas of green contour colour as shown in Figure 10. Figure 10 highlights the zones of lateral velocity switching with a green colour dotted circle.

The results shown in this paper focus on the time-averaged quantities of interest in terms of axial and lateral velocity at two measured planes for positions upstream and downstream the grid. The observations of the averaged velocity evolution for two planes of the rod bundle have been limited to the viewing area of the camera for this position. The instantaneous velocity is also available in this data, as well as parameters that can be calculated from the instantaneous velocity.

It was observed that the major velocity gradients are located at a distance of 30 mm downstream the grid for the two planes presented in this work (Plane 6 and Plane 7). The cross flow caused by the vanes is captured on these planes. The lateral velocity in Plane 7 shows that the sub-channels located in this plane have the stronger influence of the vanes with lateral velocities of 20% the average velocity in the envelope. In the other hand, the lateral velocities in Plane 6 (gaps between two adjacent rods) showed a value of 10% of the average velocity in the flow envelope. More discussion of crossflow will be provided in Section 3.2 below.

3.1.2 Detailed Cutline Results

For comparison with CFD predictions, it is convenient to define vertical cutlines that reside on vertical planes on which the PIV data is taken. In addition to Planes 6 and 7 discussed in Section 3.1.1, there was also a data plane in the rod gap on the other side of Plane 6 that is named Plane 5 (see Figure 11). Examples of vertical cutlines are shown on Figure 11. Data from vertical cutlines are compared against CFD date in another paper at this conference [9].

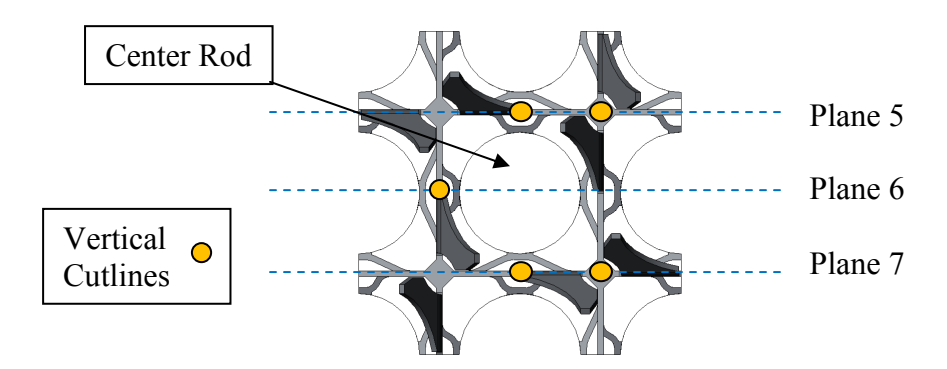


Figure 11: Top View of Vertical Cutlines

3.2 Lateral Velocity Results

The results presented in Section 3.1 focus on axial planes in the test bundle. Lateral planes are also used to get both components of the lateral velocity in the same test measurements. Figure 12 shows a full field view of average lateral velocity vectors from a lateral plane downstream of the grid. It is possible to focus in on a single subchannel for more detail investigation of the lateral velocity within a subchannel as was done in Clemson testing shown in Figure 2.

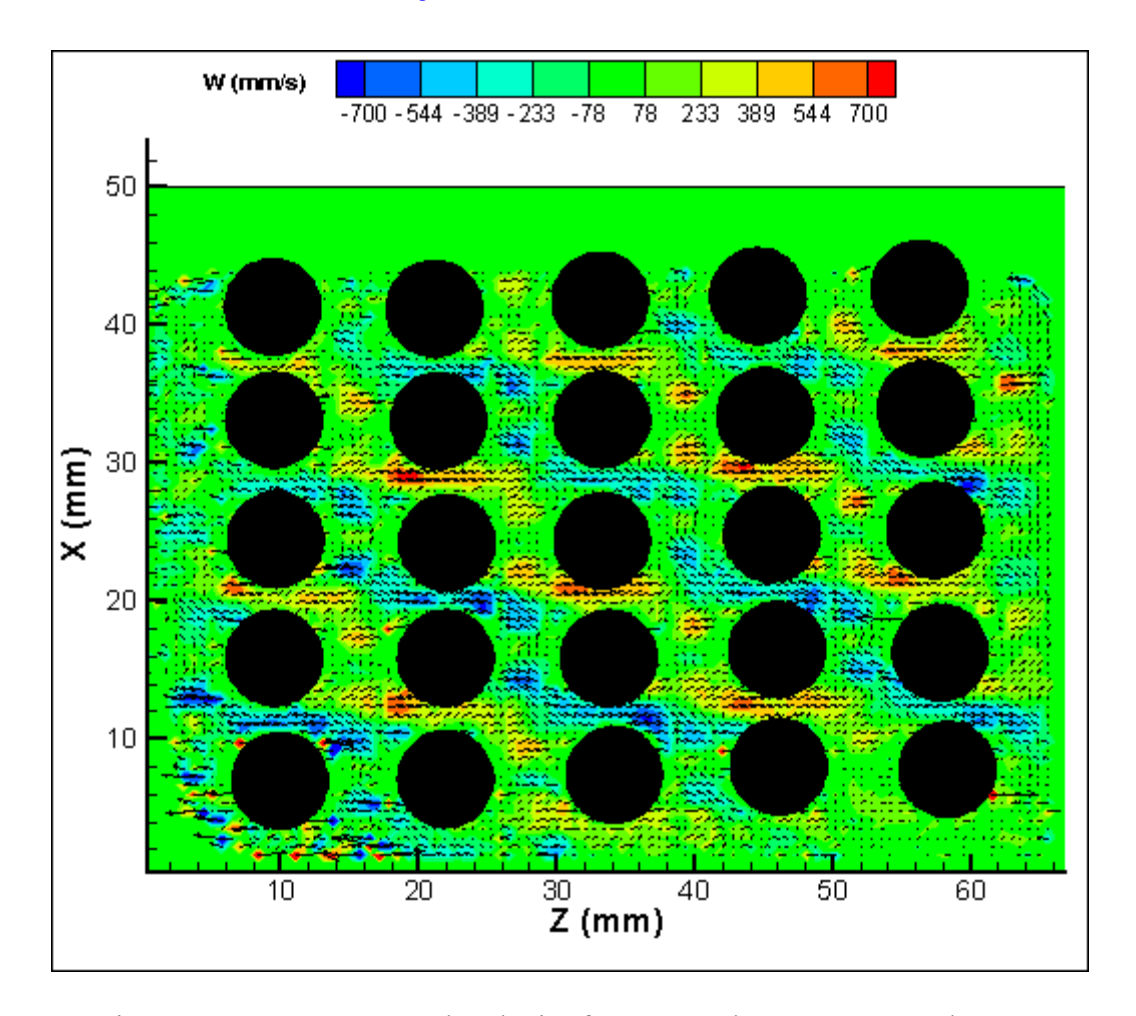


Figure 12: Average Lateral Velocity from Lateral Measurement Plane

4. Conclusions and future work

The work presented in this paper demonstrates the breadth of high spatial and temporal velocity data that can obtained for PWR grids with mixing vanes from the new test loop at Texas A&M. High quality velocity data can be obtained due to the use of (1) test rods which match the refractive index of water, (2) transparent flow housing, and (3) non-invasive PIV measurement technique. The domain of the data includes both upstream and downstream of the grid, as well as full width of the test housing. Velocity data can be obtained very close to rod and housing walls. The data can be used for full domain post-processing or as detailed information along a cutline.

The PIV data obtained from this test facility represents a step change improvement relative to the initial PIV studies performed on grids with mixing vanes. A large reason for this is the dramatic improvement in the high-speed cameras used to capture the raw data, in addition to the testing techniques listed in the paragraph above. The high spatial and temporal characteristics of this data provides a much more thorough benchmark of CFD results than were available before. Use

of this data can not only help with benchmarking of steady-state CFD simulations, but can also be used to benchmark transient CFD simulations such as LES.

5. References

- 1. McClusky, H.L., Holloway, M.V., Beasley, D.E., and Conner, M.E., 2002. "Development of Swirling Flow in a Rod Bundle Subchannel," *ASME Journal of Fluids Engineering*, Vol. 124, 747-755.
- 2. McClusky, H.L., Holloway, M.V., Conover, T.A., Beasley, D.E., Conner, M.E., and Smith III, L.D., 2003. "Mapping of the Lateral Flow Field in Typical Subchannels of a Support Grid with Vanes", *ASME Journal of Fluids Engineering*, Vol. 125, 987–996.
- 3. Holloway, M.V., McClusky, H.L., Beasley, D.E., and Conner, M.E., 2004. "The Effect of Support Grid Features on Local, Single-Phase Heat Transfer Measurements in Rod Bundles," *ASME Journal of Heat Transfer*, Vol. 126, 43-53.
- 4. Holloway, M.V., Conover, T.A., McClusky, H.L., Beasley, D.E., and Conner, M.E., 2005. "The Effect of Support Grid Design on Azimuthal Variation in Heat Transfer Coefficient for Rod Bundles," *ASME Journal of Heat Transfer*, Vol. 127, 598-605.
- 5. Holloway, M.V., Beasley, D.E., and Conner, M.E., 2008. "Single-phase Convective Heat Transfer in Rod Bundles," *Nuclear Engineering and Design*, Vol. 238, 848-858.
- 6. Conner, M.E., Baglietto, E., Elmahdi, A.M., "CFD Methodology and Validation for Single-Phase Flow in PWR Fuel Assemblies," *Nuclear Engineering and Design*, journal topical issue, Experiments and CFD Code Applications to Nuclear Reactor Safety (XCFD4NRS), Volume 240 (9), September 2010.
- 7. Okamoto, K., "Best Practice Procedures on Two-Phase Flow Experiments For CFD Validation," CFD for Nuclear Reactor Safety Applications (CFD4NRS-3) Workshop," Bethesda, Maryland, USA, September 14-16, 2010.
- 8. Dominguez-Ontiveros, E.E., Hassan, Y.A., Conner, M.E., and Karoutas, Z.E., "Experimental benchmark data for PWR rod bundle with spacer-grids," CFD for Nuclear Reactor Safety Applications (CFD4NRS-3) Workshop," Bethesda, Maryland, USA, September 14-16, 2010.
- 9. Karoutas, Z., Yan, J., Conner, M., and Mandour, A., "Advanced Thermal Hydraulic Method using 3x3 Pin Modeling," NURETH14-338, Toronto, Ontario, Canada, September 25-30, 2011.